Microfluidic reactors for visible-light photocatalytic water purification assisted with thermolysis

Ning Wang, Furui Tan, Li Wan, Mengchun Wu, and Xuming Zhang

Citation: Biomicrofluidics **8**, 054122 (2014); doi: 10.1063/1.4899883
View online: http://dx.doi.org/10.1063/1.4899883
View Table of Contents: http://scitation.aip.org/content/aip/journal/bmf/8/5?ver=pdfcov
Published by the AIP Publishing

Microfluidic reactors for visible-light photocatalytic water purification assisted with thermolysis

Ning Wang,[1,2] Furui Tan,[1,2] Li Wan,[2] Mengchun Wu,[2] and Xuming Zhang[1,2,a)]
[1]*The Hong Kong Polytechnic University Shenzhen Research Institute, Shenzhen, People's Republic of China*
[2]*Department of Applied Physics, The Hong Kong Polytechnic University, Hong Kong, China*

(Received 19 August 2014; accepted 14 October 2014; published online 24 October 2014)

Photocatalytic water purification using visible light is under intense research in the hope to use sunlight efficiently, but the conventional bulk reactors are slow and complicated. This paper presents an integrated microfluidic planar reactor for visible-light photocatalysis with the merits of fine flow control, short reaction time, small sample volume, and long photocatalyst durability. One additional feature is that it enables one to use both the light and the heat energy of the light source simultaneously. The reactor consists of a $BiVO_4$-coated glass as the substrate, a blank glass slide as the cover, and a UV-curable adhesive layer as the spacer and sealant. A blue light emitting diode panel (footprint 10 mm × 10 mm) is mounted on the microreactor to provide uniform irradiation over the whole reactor chamber, ensuring optimal utilization of the photons and easy adjustments of the light intensity and the reaction temperature. This microreactor may provide a versatile platform for studying the photocatalysis under combined conditions such as different temperatures, different light intensities, and different flow rates. Moreover, the microreactor demonstrates significant photodegradation with a reaction time of about 10 s, much shorter than typically a few hours using the bulk reactors, showing its potential as a rapid kit for characterization of photocatalyst performance. [http://dx.doi.org/10.1063/1.4899883]

I. INTRODUCTION

In recent years, intensive efforts of research and development have been invested to solve the deteriorating energy and pollution problems, among which the wastewater treatment has attracted particular attentions. Various methods such as adsorption, sedimentation, and filtration are used in industrial polluted water treatment. However, photocatalysis turns out to be a more attractive and promising method from an economical point of view because it just employs photocatalyst, dissolved oxygen, and light to decompose a wide spectrum of contaminants in wastewater at the room temperature and atmospheric pressure, without the needs for any additives and time-consuming postprocesses (e.g., filtration, sedimentation). Therefore, many types of photocatalytic reactors have been designed for water treatment, but they are still facing enormous challenge and difficulties.[1–4]

Microfluidics may find potential uses for photocatalysis but such application area remains merely a virgin land until recently.[5–7] The great success of microfluidics in many applications such as chemical analysis, biomedical assay, and drug screening has well demonstrated its remarkable capabilities in dealing with particles, fluids, and light in an integrated platform.[7–16] Thanks to its merits of flexible flow control, large surface-area-to-volume ratio, and compact size, the microfluidics could benefit the photocatalysis[16–20] in various aspects such as fast mass

a)E-mail: apzhang@polyu.edu.hk. Tel.: +852 34003258. Fax: +852 23337629.

transfer,[21–34] efficient photon transfer,[6,7,33,34] short reaction time,[6,7,21–26,34] and self-refreshing of reaction surface by running flow (and thus long photocatalyst durability).[7,34]

Based on these understandings, a number of reactors have been developed using microfluidic structures. For example, microchannels have been extensively used as the reaction chamber for photocatalysis,[21–31] the surface-area-to-volume ratio is typically in the range of 10 000–300 000 m^2/m^3,[21,22,26] at least two orders of magnitude larger than the typical value of 600 m^2/m^3 in the bulk reactors.[35–37] For this reason, significant enhancement of the reaction rate has been observed in the microchannel reactors as compared to the bulk reactors.[21–31] Recently, our group has presented an improved design-planar microreactor.[6,34] Its main body is a rectangular reaction chamber composed of a cover, a substrate, and a thin spacer (typically 100 μm-thick). The substrate has often a coating of photocatalysts (e.g., 2 μm TiO_2 nanoporous film). As compared with the microchannel reactors, the planar microreactors have large photon receiving area and large cross section (and thus high throughput). Nevertheless, most of the demonstrated microfluidic reactors are designed to use UV light from external UV sources.[6,21–34] Due to the small receiving area of microreactors (typically $< 10\,cm^2$), only a small portion of light from the UV source is utilized for photocatalytic reaction.

As an important factor for photocatalysis, thermodynamics is usually ignored or deliberately eliminated by using cooling system.[38] As reported in most work, due to the adsorption process of organic dye molecules onto the photocatalyst is endothermic, higher reaction temperature can improve the surface absorbability of photocatalyst and the oxidation activity of OH radicals, resulting in more effective decomposition of the water contaminants.[39] What is more, the photocatalytic degradation is always accompanied by self-thermolysis when the reaction temperature rises up. Therefore, it is more energy efficient if we can utilize the light and the heat from the light source at the same time.

In this work, we will present an integrated design of planar microreactor by simultaneously using light energy and its spontaneous heat energy. Compared with our previous studies[6] and the microchannel-based reactors,[21–31] two new features will be incorporated in the new microreactor—integrated light source and visible photocatalysis. The former is achieved by mounting a blue light emitting diode (LED) panel on top of the reaction chamber. The LED panel matches the reaction chamber in size and provides relatively uniform irradiation over the photocatalyst reaction surface, ensuring the best utilization of photon energy. Moreover, the direct contact of the LED panel and the reaction chamber makes it feasible to use the heat of LED panel to assist the photocatalytic reactions. The latter is done by using the visible-responsive photocatalyst bismuth vanadate ($BiVO_4$, or in short, BVO). Visible-light driven photocatalysis has long been pursued in the hope to use sunlight directly[35,36] and this work represents probably the first attempt to develop visible-responsive microreactors.

II. DESIGN AND EXPERIMENT

A. Setup of microreactor system

The setup of microreactor system is shown in Fig. 1(a), which has a blue-light LED panel mounted directly on a microreactor. In experiment, a fan and a heat sink would also be attached to the LED panel for heat dissipation to avoid overheating. Regarding the microreactor, the fabrication processes were described in our previous work.[6] It consists of two glass slides as the cover and the substrate. A 100 μm-thick UV curable adhesive layer (Norland NOA81) acts as the spacer and sealant to form a rectangular reaction chamber with volume of $10\,mm \times 10\,mm \times 100\,\mu m = 10\,\mu l$. The glass substrate is coated with the BVO film, whereas the cover uses only a blank glass slide. The blue-light LED panel has a light-emitting area (10 mm × 10 mm), which matches the area of reaction chamber. The tree-branch shaped microchannels are used to flow the solution uniformly through the reaction chamber so as to get maximum contact with the BVO film. Fig. 1(b) shows the cross-sectional view of the microreactor. The heights of the tree-branch microchannels and the reaction chamber are 50 μm and 100 μm, respectively. Fig. 1(c) shows the top view photo of the microreactor.

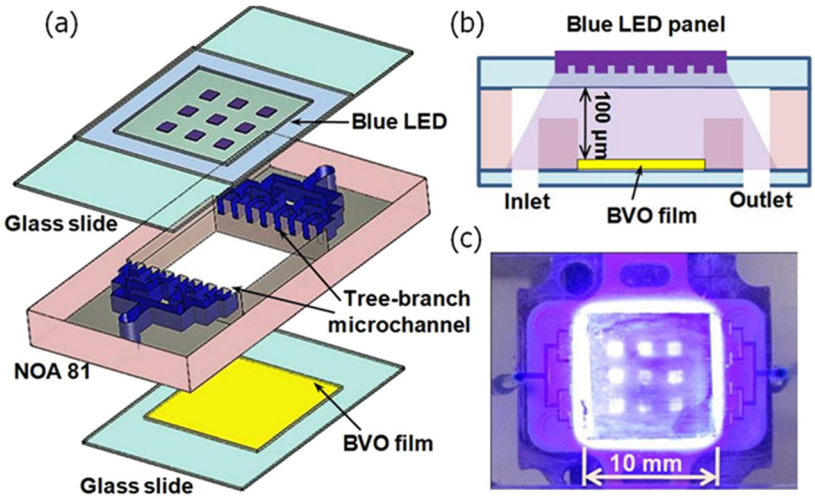

FIG. 1. Schematic diagram (a) and cross-sectional view (b) of the photocatalytic microreactor system. The microreactor consists of one $BiVO_4$-coated glass slide as the substrate, a blank glass substrate as the cover, and a 100 μm-thick UV curable adhesive layer (NOA81) as the spacer and sealant. On top of the reaction chamber (dimensions of $10 \times 10 \times 0.1\,mm^3$) is mounted a blue-light LED panel, which has a light-emitting area (10 mm × 10 mm) matching the reaction chamber. The tree-branch shaped microchannels in the NOA81 layer ensure a uniform flow of the solution through the reaction chamber. (c) Photo of the integrated microreactor system.

B. Material and instruments

$Bi(NO_3)_3{\cdot}5H_2O$ (AR, >99.9%) and NH_4VO_3 (AR, >99.9%) were purchased from Shanghai Chemical Reagent Co. Polydimethysiloxane (PDMS, DC184) was purchased from Dow Corning Co. The optical adhesive (NOA81) was purchased from Norland Products. Other chemicals including methylene blue (MB) reagent, polyethylene glycol (PEG 20000), and detergent (Triton X-100) were purchased from Sigma-Aldrich Co. MB solutions with different concentrations were prepared by dissolving in deionized water. The blue-light LED panel was purchased from Shenzhen Getian Co.

The standard UV lithography was used to fabricate the PDMS mold and the UV lamp to cure the NOA 81 adhesive.[6] Characterization of the synthesized BVO nanoparticles was conducted using a field-emission scanning electron microscope (FE-SEM) (Bruker, D8 Advanced), X-ray diffraction (XRD) (JEOL, JSM-633F), and UV-Vis spectrophotometer (UV-2550, Shimadzu). To examine the concentration change between the original and the degraded MB solution, the absorption spectra were analyzed by the same UV-Vis spectrophotometer.

C. Fabrication of $BiVO_4$ nanoparticles and thin film

Nanosized BVO particles were synthesized by a solid-phase precipitation preparation method assisted with ultrasonic agitation.[40] First, aqueous solutions of $Bi(NO_3)_3{\cdot}5H_2O$ and NH_4VO_3 in 1:1 molar ratio were mixed. The pH value of the final suspension was adjusted to about 7 by adding $NH_3{\cdot}H_2O$. Then, the mixture was stirred for 1 h at room temperature. Afterward, the mixture was subject to ultrasonic agitation (100 W) at room temperature in open air for several hours. Next, the yellow precipitates were centrifuged, washed by de-ionized water and absolute ethanol, and then dried at 60 °C in air for 10 h. The obtained powders were subsequently calcined at 450 °C for 2 h to produce crystalline products.

To enhance the photocatalytic performance of the microreactor, a nano-porous BVO thin film was fabricated to increase its specific surface area. The grinded powders (6 g) were slowly dispersed in deionized water (60 ml) containing acetylacetone (0.2 ml) to prevent reaggregation of the particles. Then, Triton X-100 (0.1 ml) was added to spread the colloid on the substrate. Finally, PEG 20000 (0.6 g) was added into the aqueous solution under ultrasonic agitation for about 2 h. As a result, the catalyst colloid was formed. Next, a painting method was used to

form a BVO thin film on a clean glass slide and dried at 80 °C. Finally, the BVO thin film was annealed under 500 °C for 2 h in air.

D. Efficiency test of the integrated device

Before the degradation experiment, the LED panel was driven by a DC power supplier and its optical properties were characterized. The light intensity of the LED was measured by a Reference Solar Cell and Meter (91150 V, Newport) and the emission wavelength was measured by an integrating sphere (Labsphere). The temperature of microreactor is measured by a thermocouple. Fig. 2 plots the emission power density P of the LED and the reaction temperature T with respect to the driving voltage V. The black round points represent the power density P and follow closely a linear relationship $P = 65.7(V - 8.8)$, here P in the unit of mW/cm^2, V in volt. And the change of reaction temperatures is also plotted as shown with the blue line. The inset of Fig. 2 shows the emission spectrum of the LED. A single peak appears at 402 nm with a linewidth of 20 nm. The stability of the LED panel was also tested and the result showed a decrease of the power density by <2% in about 2 h. The MB solution as the original reagent was introduced into the microreactor by a syringe pump (TS2–60, Longer). The initial concentration was set to 3×10^{-5} mol/l. The photodegraded MB solution was collected from the outlet.

III. EXPERIMENTAL RESULTS

A. Material characterization

The phase and composition of the BVO sample were characterized by XRD, as shown in Fig. 3. The diffraction peaks agree well with those of the pure monoclinic BVO according to the JCPDS No. 14–0688. This shows that the synthesized nanosized BVO is in pure monoclinic phase and possesses high photoreactivity.

Since the optical absorption of the photocatalyst is one of the determining factors of photoreactivity,[41] UV-vis diffuse reflectance spectrum (DRS) of the synthesized nanosized BVO samples was also investigated. The result is shown in the inset of Fig. 3. It can be seen that the BVO has strong absorption in visible-light region (<500 nm) and in the UV light region. The absorbance at 402 nm is 86% of the peak absorbance at 284 nm. This implies that the blue-light LED panel can be used as the photocatalytic light source.

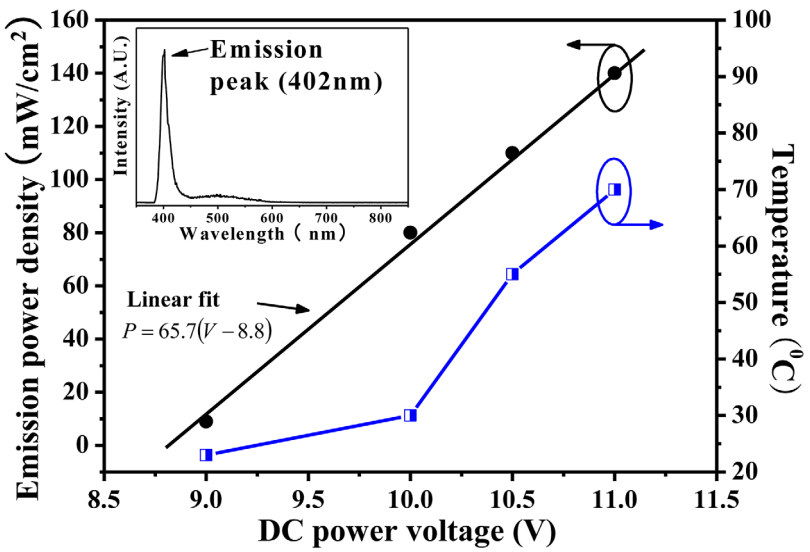

FIG. 2. Emission power density of the blue-light LED panel and reaction temperature as a function of the driving voltage. The inset shows the LED emission spectrum.

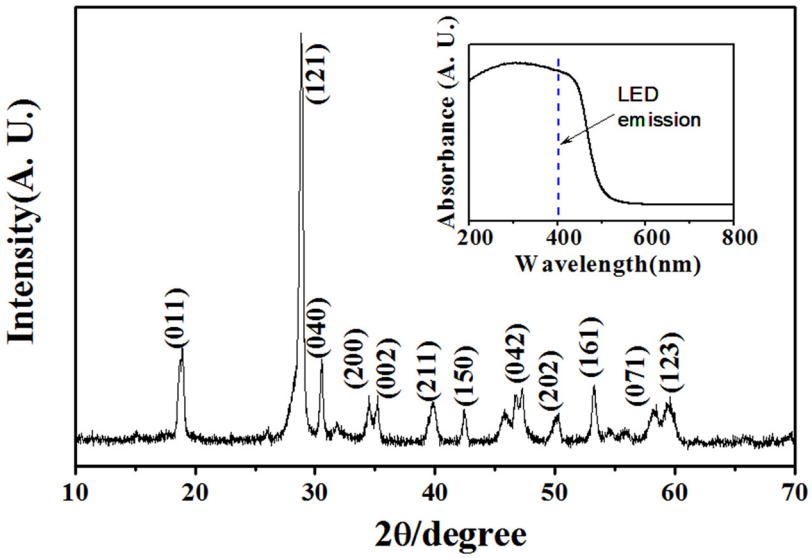

FIG. 3. X-ray diffraction (XRD) spectrum of the synthetic nanosized $BiVO_4$. The inset shows the UV-vis diffuse reflectance spectrum.

The morphology and microstructure of the BVO samples were investigated by scanning electron microscopy (SEM). Fig. 4 shows the SEM image of the BVO film. It is composed of porous structure and nanosized particles with an average size of about 80–100 nm. The inset in Fig. 4 shows the cross section of the BVO film. The thickness is about 1.5 μm, which is chosen for high photoreactivity. Through experimental studies, we have found that the photoreactivity increases with the BVO film thickness and tends to saturate when the thickness of the BVO film goes beyond 600 nm. This is reasonable since the photocatalytic reaction only occurred on the surface of the nanosized photocatalyst. The thickness of 1.5 μm ensures the BVO film works in its highest photoreactivity.

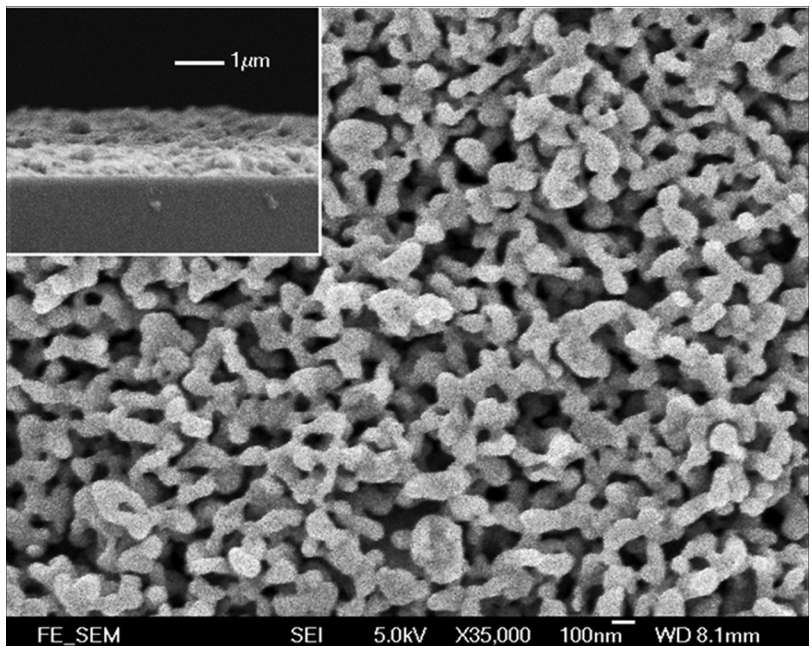

FIG. 4. Scanning electron micrograph (SEM) of the $BiVO_4$ thin film, which is composed of porous structures formed by the nanosized $BiVO_4$. The inset shows the cross section of the $BiVO_4$ film. The thickness is about 1.5 μm.

B. Effect of flow rate

In the microreactor system, the flow rate is one of the major factors that affect the photocatalytic reaction efficiency. The flow rate is related to the effective residence time of the MB solution in the reaction chamber by the relationship

$$\text{Effective residence time} = \frac{\text{Chamber volume}}{\text{Flow rate}}. \tag{1}$$

To investigate the effect of the flow rate, the solutions were pumped at 37.5, 50, 75, and 150 μl/min, respectively. The corresponding effective residence time (i.e., the reaction time) is 16, 12, 8, and 4 s, respectively. The blue-light LED is driven at a constant 11 V (corresponding to a power density of 140 mW/cm^2). For control experiment, a similar hollow microreactor without the nanoporous BVO film was also tested under the same conditions of flow rates and light intensity. Without the BVO film, the decomposition comes mostly from the thermolysis of MB.

In data analysis, the reaction rate constant can be deduced from the degradation in the reactor through the relationship[35]

$$\ln\left(\frac{C_0}{C}\right) \propto kt, \tag{2}$$

where ln is the logarithm of natural base, k is the reaction rate constant, t is the effective reaction time, and C_0 and C represent the initial concentration and the concentration after degradation, respectively. Using this relationship, the reaction rate constants of the microreactor system can be calculated and compared. The experimental results are plotted in Fig. 5. The data points and the error bars represent the averaged values and the standard deviations of three measurements, respectively. A linear fit of the tested data for the control experiment gives a slope of $k_{control} = 0.007\ \text{s}^{-1}$ owing to the thermolysis. In comparison, the microreactor yields $k = 0.031\ \text{s}^{-1}$, more than 4 times of that of the control. This shows the BVO film works effectively, though not as good as expected.

The inset in Fig. 5 plots the reaction rate with respect to the effective residence time. The data points are the averaged values. Here, the reaction rate represents how many percents of the MB are degraded over a unit period of time. It can be observed that the maximum reaction rate

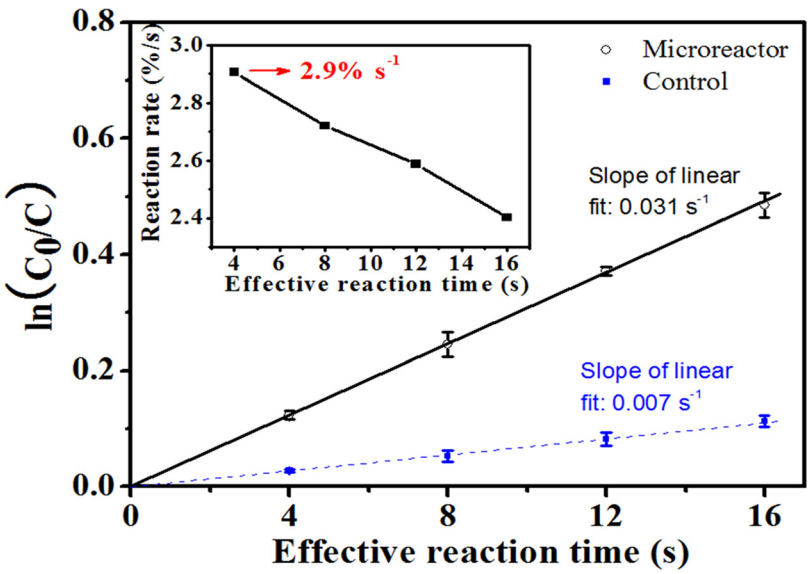

FIG. 5. Napierian logarithm of the degradation as a function of the effective residence time. The inset shows the reaction rate at different flow rates when the blue light LED panel is driven at 11 V.

2.9% s^{-1} corresponds to the shortest residence time 4 s (i.e., the largest flow rate 150 μl/min). The reason for this behavior is not straightforward but can be explained by considering the mass transfer efficiency and the oxygen availability during the reaction.[6]

C. Effects of light source intensity and temperature

The light intensity is obviously a major factor that affects the photocatalytic performance of the microreactor system. The intensity of the LED emission is varied by adjusting the driving voltage from 9 to 11 V. The curves at different flow rates are plotted in Fig. 6. It can be seen that the degradation percentage increases with stronger light power density. This is reasonable since more photons would increase the photoreaction. Here, the degradation percentage τ is defined as $\tau = (1 - C/C_0) \times 100\%$, it is also called *conversion* in some articles.[42] When comparing the curves of different flow rates, one can see that high flow rate leads to a low degradation percentage. This is because faster flow causes shorter residence time in the reaction chamber (and thus shorter reaction time). These results show clearly that the microreactor system enables easy control of the photocatalysis by adjusting the flow rate and the light intensity of LED. All the error bars shown in Fig. 6 were calculated by measuring only one microreactor for 3 to 4 times. The whole measurement took over 40 h, while the BVO film in the reaction chamber degraded by only about 2%. This well demonstrates the long durability of photocatalyst film.

Another important factor, though often ignored, is the reaction temperature. Although a heat sink is fixed on the LED panel, the generated heat still cannot dissipate fast enough, especially under high controlled voltage. Therefore, the reaction temperature in the reaction chamber should be higher than room temperature. As mentioned above, this would affect the photocatalysis.[39] Because of the small dimensions of reaction chamber, it is difficult to measure the inner temperature directly. As an approximation, the temperature of the upper surface of reaction chamber is always monitored by a thermocouple during the experiment. The temperature measures to be close to room temperature under 9 V, ~30 °C under 10 V, ~55 °C under 10.5 V, and ~70 °C under 11 V (see Fig. 2). As a control experiment to investigate the sole effect of temperature, we used a hot plate to heat the microreactor up to 80 °C (dark environment, no light). The measured reaction rate constants are plotted in Fig. 7(a) using the blue dashed line. By deducing for degradation rates in Fig. 6, the results when the light is on are plotted using the solid red line, which include the combined effect of light and heat generated by visible LED panel. It can be seen from Fig. 7(a) that

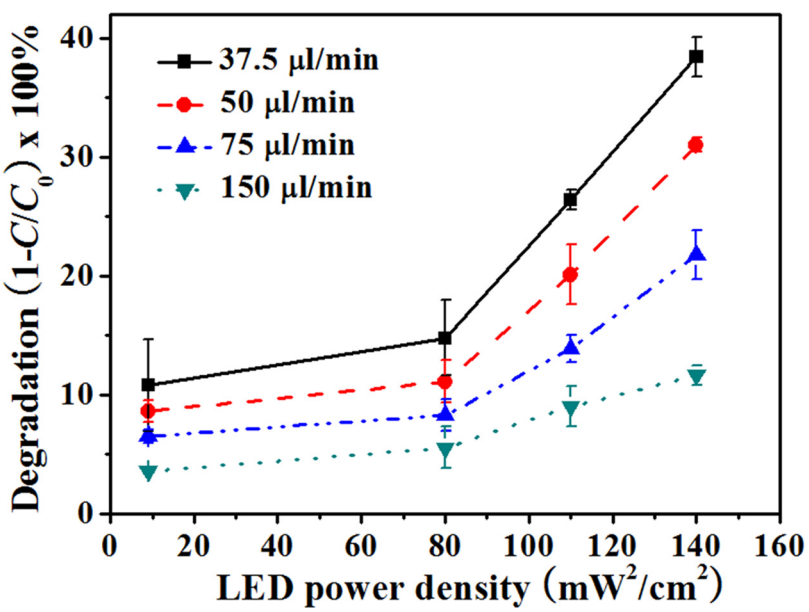

FIG. 6. Influence of the light intensity on the degradation percentage at different flow rates.

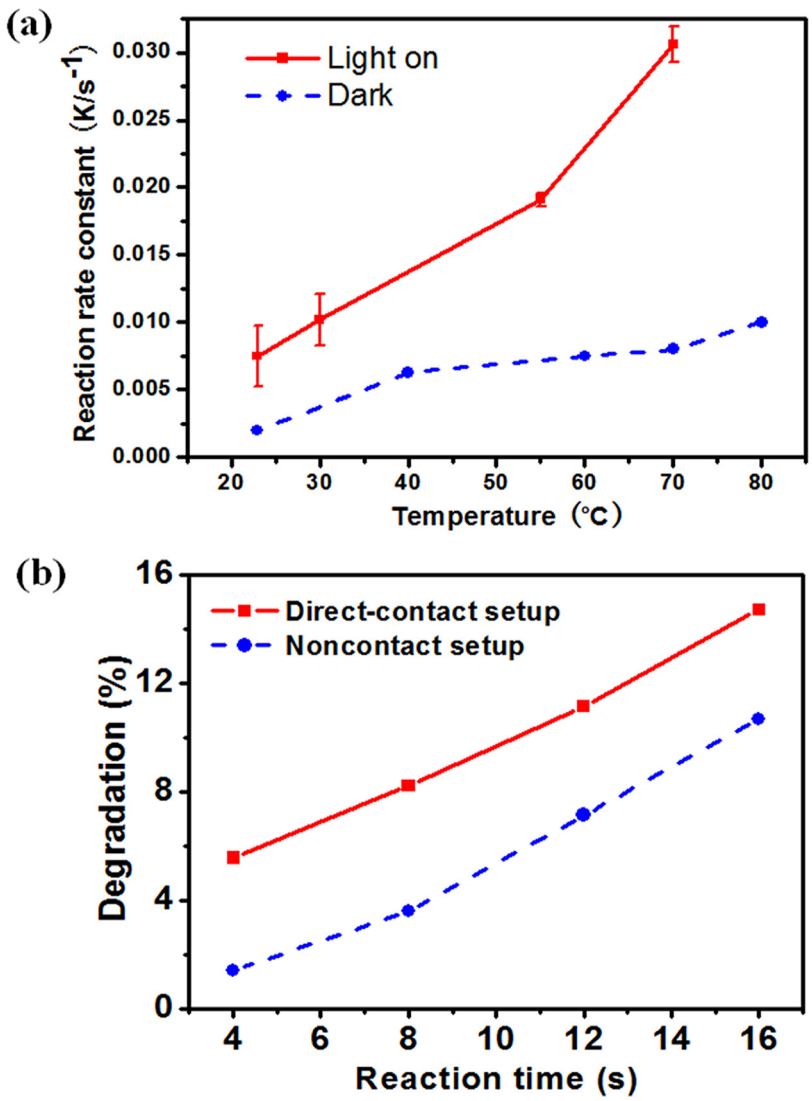

FIG. 7. (a) Influence of the temperature on the reaction rate constant at the flow rate of 37.5 μl/min; (b) comparison of the degradation rates with and without the heat. The direct-contact LED setup has similar irradiation densities with the noncontact LED setup, but the former is affected by the heat of LED, while the latter is not.

the thermolysis has an obvious contribution (e.g., degradation percentage $>$ 10% at 60 °C), though the combined effect of light and heat yields much larger value.

To obtain the direct proof of the contribution of thermolysis, another control experiment was conducted. The reactor was fixed about 1 cm above the LED surface (named as the noncontact setup). With the aid of an air fun, the reaction temperature could be maintained close to the room temperature. The supply voltage was set at 11.5 V so that the irradiation density on the reaction chamber was nearly the same as that of the direct-contact setup under 10 V. The experimental results were plotted in Fig. 7(b). It can be seen that the photodegradation rates of the direct-contact setup are 4%–6% larger than that of the noncontact setup. This difference indicates the contribution of heat to the MB degradation.

Dissolved oxygen in water is supposed to be an additional key factor that determines the decomposition rate of MB. But when the temperature goes beyond 80 °C, air bubbles come out in the reaction chamber, with the repeated growth and collapse of bubbles. This may be attributed to the degassing of dissolved air in the water. Once the bubbles appear, they would also affect the flow in the chamber. This is why the upper limit is set to 70 °C in the control experiment.

TABLE I. Apparent quantum efficiencies of the microreactor system at different LED power densities and different residence times.

LED driving voltage (V)	Power density (mW/cm^2)	Reaction temperature (°C)	Apparent quantum efficiency η			
			16 s	12 s	8 s	4 s
9.0	9.0	23	0.043%	0.061%	0.10%	0.23%
10.0	80	30	0.007%	0.009%	0.015%	0.040%
10.5	110	55	0.009%	0.012%	0.018%	0.047%
11.0	140	70	0.010%	0.014%	0.022%	0.048%

D. Light utilization efficiency

Apparent quantum efficiency η can be used to evaluate the efficiency of the photocatalytic microreactor. It is defined by $\eta = 102N_{mol}/N_{photon}$, where N_{mol} is the number of reacted molecules and N_{photon} the number of photons absorbed by the photocatalyst or reactants.[6] The value 102 is because one MB molecule needs 102 electrons for total mineralization.[6] With this relationship, the apparent quantum efficiencies under the LED power densities can be calculated as listed in Table I. For instance, the number of photons that arrive at the BVO film surface under 140 mW/cm^2 is 2.8×10^{17} photons/s,[43] and the maximum reaction rate of 2.9%/s corresponds to the decomposition of 1.3×10^{12} molecules/s of MB. In this case, the apparent quantum efficiency is $\eta = 0.048\%$. Similarly, the apparent quantum efficiencies for the other conditions can be calculated. It is seen from Table I that the apparent quantum efficiency reaches its maximum of 0.23% at the weakest power density of 9 mW/cm^2. This is reasonable since the reaction rate constant k follows approximately $k \propto \sqrt{P}$, here P is the optical power density. As a result, the apparent quantum efficiency is proportional to $1/\sqrt{P}$ and thus weaker power density enjoys higher apparent quantum efficiency. It is noted that in Table I the apparent quantum efficiencies for the other three high-intensity conditions do not follow the $1/\sqrt{P}$ relationship. Oppositely, the apparent quantum efficiency increases with P. This is reasonable if the effect of thermolysis is taken in account. At higher intensity, the temperature goes higher and thus the thermolysis becomes stronger.

IV. DISCUSSIONS

This microreactor has a very limited throughput (e.g., 9 ml/h for the flow rate of 150 μl/min) and may not be used directly for practical water purification applications (typically threshold throughput > 1000 l/h). Nevertheless, it may be used as a rapid test kit to quantify the performance of photocatalytic materials[27] and to optimize the operational conditions. In this microreactor, significant degradation can be obtained within about 10 s, this is impressive as compared to the typically a few hours in bulk photocatalytic reactors.[4,19,23,24,35,37,44] In addition, this microreactor requires only a few millilitres of sample due to the small reaction chamber. This is useful when the photocatalysts and the sample solution are costly. Moreover, the microreactor provides fine control of many conditions of reactions such as flow rate (affecting the mass transfer) and flow condition (laminar or turbulent), making it a useful platform to study the kinetics and detailed mechanisms of photocatalytic reactions.[29,30] Moreover, many well-developed microfluidic manipulation and detection techniques could be incorporated into the microreactors for in-line monitoring of the intermediate and final products.[16,30,45]

V. CONCLUSIONS

A photocatalytic microreactor system was constructed by directly mounting a blue-light LED panel on a microfluidic planar reactor, which enables to make use of both the heat and the light energy for organic degradation. Experimental studies have shown that the microreactor facilitates the control of photocatalytic process by adjusting the LED light intensity and the flow rate. These

correspond to the control of two important photocatalytic factors: the photon transfer and the mass transfer. The influence of different reaction temperatures to photocatalysis performance of microreactor has also been investigated. Along with other features such as short reaction time and small sample volume, the microreactor system could provide a versatile tool to study the reaction kinetics of photocatalysis and a rapid kit to characterize the performance of photocatalysts.

ACKNOWLEDGMENTS

This work was partially supported by National Science Foundation of China (No. 61377068) and Research Grants Council (RGC) of Hong Kong (N_PolyU505/13 and PolyU 5327/11 E). The authors would like to thank The Hong Kong Polytechnic University for the grants G-YN07, 1-ZVAW, A-PL16, 1-ZE14, and A-PM21.

[1]M. N. Chong, B. Jin, C. W. K. Chow, and C. Saint, Water Res. **44**, 2997–3027 (2010).
[2]R. Dillert, S. Vollmer, M. Schober, J. Theurich, D. Bahnemann, H.-J. Arntz, K. Pahlmann, J. Wienefeld, T. Schmedding, and G. Sager, Chem. Eng. Technol. **22**, 931 (1999).
[3]C. McCullagh, N. Skillen, M. Adams, and P. K. J. Robertson, J. Chem. Technol. Biotechnol. **86**, 1002–1017 (2011).
[4]T. Van Gerven, G. Mul, J. Moulijn, and A. Stankiewicz, Chem. Eng. Process. **46**, 781–789 (2007).
[5]D. Erickson, D. Sinton, and D. Psaltis, Nat. Photonics **5**, 583–590 (2011).
[6]L. Lei, N. Wang, X. M. Zhang, Q. D. Tai, D. P. Tsai, and H. L. W. Chan, Biomicrofluidics **4**, 043004 (2010).
[7]N. Wang, X. M. Zhang, Y. Wang, W. X. Yu, and H. L. W. Chan, Lab Chip **14**, 1074–1082 (2014).
[8]G. M. Whitesides, Nature **442**, 368–373 (2006).
[9]P. S. Dittrich and A. Manz, Nat. Rev. Drug Discovery **5**, 210–218 (2006).
[10]W. Z. Song, X. M. Zhang, A. Q. Liu, C. S. Lim, P. H. Yap, and H. M. M. Hosseini, Appl. Phys. Lett. **89**, 203901 (2006).
[11]C. Monat, P. Domachuk, and B. J. Eggleton, Nat. Photonics **1**, 106–114 (2007).
[12]A. Q. Liu, H. J. Huang, L. K. Chin, Y. F. Yu, and X. C. Li, J. Anal. Bioanal. Chem. **391**, 2443–2452 (2008).
[13]L. K. Chin, A. Q. Liu, C. S. Lim, C. L. Lin, T. C. Ayi, and P. H. Yap, Biomicrofluidics **4**, 024107 (2010).
[14]Y. Yang, A. Q. Liu, L. K. Chin, X. M. Zhang, D. P. Tsai, C. L. Lin, C. Lu, G. P. Wang, and N. I. Zheludev, Nat. Commun. **3**, 651 (2012).
[15]X. Fan and I. M. White, Nat. Photonics **5**, 591–597 (2011).
[16]G. V. Casquillas, C. Fu, M. Le Berre, J. Cramer, S. Meance, A. Plecis, D. Baigl, J.-J. Greffet, Y. Chen, M. Piel, and P. T. Tran, Lab Chip **11**, 484–489 (2011).
[17]*Photocatalytic Purification and Treatment of Water and Air*, edited by D. F. Ollis and H. Al-Ekabi (Elsevier, Amsterdam, 1993).
[18]J. M. Herrmann, Catal. Today **53**, 115–129 (1999).
[19]M. R. Hoffmann, S. T. Martin, W. Choi, and D. W. Bahnemann, Chem. Rev. **95**, 69–96 (1995).
[20]J. Hegyi and O. Horváth, in *From Colloids to Nanotechnology*, Progress in Colloid and Polymer Science Vol. 125 (Springer, 2004), pp. 10–16.
[21]R. Gorges, S. Meyer, and G. Kreisel, J. Photochem. Photobiol. A **167**, 95–99 (2004).
[22]H. Lindstrom, R. Wootton, and A. Iles, AIChE J. **53**, 695–702 (2007).
[23]H. Lu, M. A. Schmidt, and K. F. Jensen, Lab Chip **1**, 22–28 (2001).
[24]R. C. R. Wootton, R. Fortt, and A. J. de Mello, Org. Process Res. Dev. **6**, 187–189 (2002).
[25]X. Li, H. Wang, K. Inoue, M. Uehara, H. Nakamura, M. Miyazaki, E. Abe, and H. Maeda, Chem. Commun. **2003**(8), 964–965.
[26]G. Takei, T. Kitamori, and H. B. Kim, Catal. Commun. **6**, 357–360 (2005).
[27]H. Zhang, J.-J. Wang, J. Fan, and Q. Fang, Talanta **116**, 946–950 (2013).
[28]W. Ehrfeld, V. Hessel, and H. Löwe, *Microreactors: New Technology for Modern Chemistry* (VCH/Wiley, Weinheim, Germany, 2000).
[29]K. F. Jensen, Chem. Eng. Sci. **56**, 293–303 (2001).
[30]St. Walter, St. Malmberg, B. Schmidt, and M. A. Liauw, Catal. Today **110**, 15–25 (2005).
[31]P. Watts and C. Wiles, Chem. Commun. **2007**(5), 443–467.
[32]L. Li, R. Chen, X. Zhu, H. Wang, Y. Z. Wang, Q. Liao, and D. Wang, ACS Appl. Mater. Interfaces **5**, 12548–12553 (2013).
[33]S. S. Ahsan, A. Gumus, and D. Erickson, Lab Chip **13**, 409–414 (2013).
[34]N. Wang, X. M. Zhang, B. L. Chen, W. Z. Song, N. Y. Chan, and H. L. W. Chan, Lab Chip **12**, 3983–3990 (2012).
[35]T. Oyama, A. Aoshima, S. Horikoshi, H. Hidaka, J. Zhao, and N. Serpone, Sol. Energy **77**, 525–532 (2004).
[36]D. Robert and S. Malato, Sci. Total Environ. **291**, 85–97 (2002).
[37]S. Malato, J. Blanco, A. Vidal, D. Alarcón, M. I. Maldonado, J. Cáceres, and W. Gernjak, Sol. Energy **75**, 329–336 (2003).
[38]B. Liu, X. Zhao, C. Terashima, A. Fujishima, and K. Nakata, Phys. Chem. Chem. Phys. **16**, 8751–8760 (2014).
[39]N. A. Oladoja, C. O. Aboluwoye, Y. B. Oladimeji, A. O. Ashogbon, and I. O. Otemuyiwa, Desalination **227**, 190–203 (2008).
[40]M. Shang, W. Z. Wang, L. Zhou, S. M. Sun, and W. Z. Yin, J. Hazard. Mater. **172**, 338–344 (2009).
[41]J. Tang, Z. Zou, and J. Ye, Angew. Chem., Int. Ed. **43**, 4463–4466 (2004).
[42]J.-M. Herrmann, J. Photochem. Photobiol. A **216**, 85–93 (2010).
[43]R. E. Bird, R. L. Hulstrom, and L. J. Lewis, Sol. Energy **30**, 563–573 (1983).
[44]O. M. Alfano, D. Bahnemann, A. E. Cassano, R. Dillert, and R. Goslich, Catal. Today **58**, 199–230 (2000).
[45]T. J. Johnson, D. Ross, and L. E. Locascio, Anal. Chem. **74**, 45–51 (2002).